Structural Studies on Phenyl Bismuth Halides and Halogenoanions†

William Clegg,[a] R. John Errington,[a] George A. Fisher,[a] David C. R. Hockless,[a] Nicholas C. Norman,*,[a] A. Guy Orpen*,[b] and Susan E. Stratford[b]
[a] *Department of Chemistry, The University, Newcastle upon Tyne NE1 7RU, UK*
[b] *Department of Chemistry, The University, Bristol BS8 1TS, UK*

Structural studies by X-ray crystallography have been carried out for a range of phenyl bismuth halides and halogenoanions. The complexes [BiPhBr$_2$(thf)] **1** and [BiPhI$_2$(thf)] **2** (thf = tetrahydrofuran) form one-dimensional polymeric chains with a single asymmetrically-bridging halide between each pair of adjacent bismuth atoms. The co-ordination geometry around the bismuth centre is that of a square-based pyramid with the phenyl group in the apical position and two *cis* halides, a bridging halide from an adjacent monomer unit and a thf ligand in the basal plane. Addition of [NEt$_4$]I to **2** affords the ionic species [NEt$_4$]$_2$[Bi$_2$Ph$_2$I$_6$]·Et$_2$O **3** which contains the discrete dimeric [Bi$_2$Ph$_2$I$_6$]$^{2-}$ anion. This anion comprises two edge-shared square-based pyramids with an angle of 105.2° between the basal planes. As with **1** and **2**, the phenyl group occupies the apical site with the basal sites around each bismuth occupied by two terminal and two bridging iodides. The complex [BiPh$_2$Br(thf)] **5** is monomeric and has an equatorially vacant trigonal-bipyramidal co-ordination geometry around the bismuth centre in which the phenyl groups occupy the equatorial sites and the bromine and thf ligand the axial sites. The structure of [PPh$_4$][BiPh$_2$Br$_2$] **6** contains monomeric [BiPh$_2$Br$_2$]$^-$ anions with a geometry similar to that found in **5**. Comparisons are made, where appropriate, with related tellurium(IV) compounds, and the nature of the bonding in the complexes is discussed particularly with regard to the details of the secondary, intermolecular bonds observed in the structures of **1**–**3**.

Organobismuth(III) halides have been known for many years and have been reviewed several times[1] but to the best of our knowledge, very few structural studies have been reported. The structural chemistry of bismuth is, however, an area of increasing interest, not least because of the importance of this element in oxidation catalysis and in some of the new copper oxide based superconductors. Herein, we describe the results of a number of structure determinations of phenyl bismuth(III) halides and halogenoanions, which demonstrate the appreciable Lewis acidity of bismuth(III), and the importance of secondary bonding, as discussed by Alcock,[2] in the structural chemistry of this element.

Results and Discussion

The compound BiPhBr$_2$ was prepared by the method of Gilman *et al.*[3] from the reaction between BiPh$_3$ and two equivalents of BiBr$_3$ in Et$_2$O. Both reactants are soluble in this solvent but BiPhBr$_2$ is almost completely insoluble and precipitates immediately and quantitatively as a pale yellow solid. Dissolution in tetrahydrofuran (thf) and crystallisation by solvent diffusion with hexanes afforded pale yellow crystals of the complex [BiPhBr$_2$(thf)] **1**. The structure of **1** was established by X-ray crystallography, the results of which are shown in Figs. 1 and 2. Selected bond distances and angles are given in Table 1 and atomic positional parameters in Table 2. As is evident from Fig. 2, compound **1** comprises a bromide-bridged, polymeric structure. The co-ordination geometry around each bismuth is close to an ideal square-based pyramid with the phenyl group occupying the apical position. The Bi–C distance is 2.281(9) Å which is comparable to that found in BiPh$_3$ (av. 2.24 Å),[4] Bi$_2$Ph$_4$ (av. 2.27 Å)[5] and a range of phenylbismuth-transition-metal carbonyl complexes recently described by Cassidy and Whitmire.[6] In the basal plane are the oxygen atom of a co-ordinated thf molecule [Bi–O 2.671(8) Å] and three bromines, two of which act as bridges to adjacent bismuth centres; the bismuth lies only 0.040(2) Å below the mean plane of the basal atoms. Atom Br(1) is terminal and has the shortest bond distance [2.684(1) Å]; Br(2) is bridging but asymmetrically, with a distance of 2.825(1) Å to Bi and 3.038(1) Å to the adjacent and symmetry related Bi(d). The co-ordination around Br(2) is

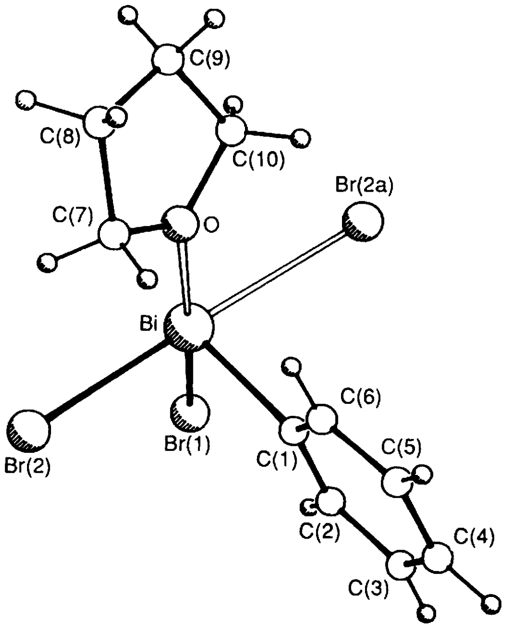

Fig. 1 A view of the structure of the monomeric unit of **1** showing the atom numbering scheme adopted

---

† *Supplementary data available:* see Instructions for Authors, *J. Chem. Soc., Dalton Trans.*, 1992, Issue 1, pp. xx–xxv.

Table 1 Selected bond lengths (Å) and angles (°) for compound **1**

Bi–Br(1)	2.684(1)	Bi–Br(2)	2.825(1)
Bi–Br(2a)	3.038(1)	Bi–O	2.671(8)
Bi–C(1)	2.281(9)		
Br(1)–Bi–Br(2)	93.7(1)	Br(1)–Bi–C(1)	93.9(2)
Br(2)–Bi–C(1)	89.9(2)	Br(1)–Bi–O	177.4(2)
Br(2)–Bi–O	85.4(2)	C(1)–Bi–O	88.5(3)
Br(1)–Bi–Br(2a)	93.5(1)	Br(2)–Bi–Br(2a)	171.2(1)
C(1)–Bi–Br(2a)	84.4(2)	O–Bi–Br(2a)	87.7(2)
Bi–Br(2)–Bi(d)	105.1(1)		

Symmetry operations for Table 1 and Figs. 1 and 2: (a) $-x, \frac{1}{2} + y, \frac{1}{2} - z$; (b) $x, 1 + y, z$; (c) $-x, \frac{3}{2} + y, \frac{1}{2} - z$; (d) $-x, -\frac{1}{2} + y, \frac{1}{2} - z$; (e) $x, -1 + y, z$.

Table 2 Atomic coordinates (× 10^4) for compound **1**

Atom	x	y	z
Bi	66(1)	1961(1)	2400(1)
Br(1)	1699(1)	1909(1)	1104(1)
Br(2)	1866(1)	−357(1)	3106(1)
C(1)	1833(11)	3551(10)	3035(6)
C(2)	3104(12)	4131(12)	2662(6)
C(3)	4118(13)	5161(13)	3043(7)
C(4)	3813(13)	5585(13)	3812(7)
C(5)	2530(14)	4952(15)	4183(7)
C(6)	1565(14)	3923(13)	3771(6)
O	−1622(9)	1898(10)	3669(4)
C(7)	−1387(16)	1047(15)	4370(7)
C(8)	−3058(26)	886(25)	4661(12)
C(9)	−4146(17)	1757(18)	4188(9)
C(10)	−3144(12)	2621(13)	3650(7)

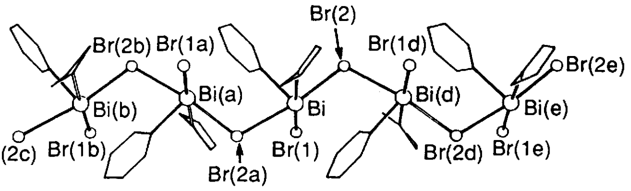

Fig. 2 A view of part of the bromide-bridged polymeric structure of **1**

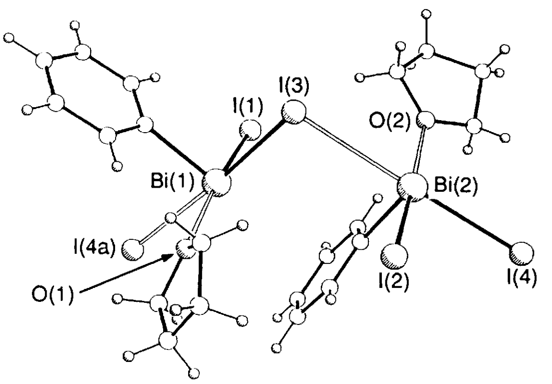

Fig. 3 A view of the crystallographic repeat unit of **2**, comprising two monomeric units, showing the atom numbering scheme adopted

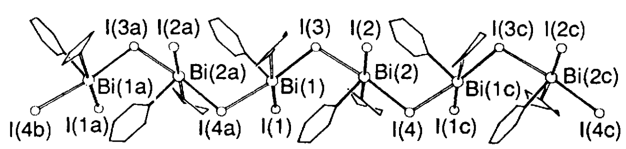

Fig. 4 A view of part of the iodide-bridged polymeric structure of **2**

Table 3 Selected bond lengths (Å) and angles (°) for compound **2**

Bi(1)–I(1)	2.882(2)	Bi(1)–I(3)	3.056(2)
Bi(1)–O(1)	2.808(17)	Bi(1)–C(11)	2.239(16)
Bi(1)–I(4a)	3.227(2)	Bi(2)–I(2)	2.892(2)
Bi(2)–I(3)	3.211(2)	Bi(2)–I(4)	3.079(2)
Bi(2)–O(2)	2.813(18)	Bi(2)–C(21)	2.242(16)
I(1)–Bi(1)–I(3)	94.8(1)	I(1)–Bi(1)–O(1)	175.0(4)
I(3)–Bi(1)–O(1)	85.9(4)	I(1)–Bi(1)–C(11)	94.8(4)
I(3)–Bi(1)–C(11)	88.6(4)	O(1)–Bi(1)–C(11)	90.1(5)
I(1)–Bi(1)–I(4a)	91.1(1)	I(3)–Bi(1)–I(4a)	172.8(1)
O(1)–Bi(1)–I(4a)	88.6(4)	C(11)–Bi(1)–I(4a)	86.8(4)
I(2)–Bi(2)–I(3)	93.5(1)	I(2)–Bi(2)–I(4)	93.9(1)
I(3)–Bi(2)–I(4)	171.8(1)	I(2)–Bi(2)–O(2)	174.9(4)
I(3)–Bi(2)–O(2)	83.0(4)	I(4)–Bi(2)–O(2)	89.8(4)
I(2)–Bi(2)–C(21)	96.7(4)	I(3)–Bi(2)–C(21)	87.1(4)
I(4)–Bi(2)–C(21)	88.6(4)	O(2)–Bi(2)–C(21)	86.9(5)
Bi(1)–I(3)–Bi(2)	100.3(1)	Bi(2)–I(4)–Bi(1c)	101.1(1)

Symmetry operations for Table 3 and Figs. 3 and 4: (a) $x, -1 + y, z$; (b) $x, -2 + y, z$; (c) $x, 1 + y, z$.

bent [Bi–Br(2)–Bi(d) 105.1(1)°] but of more interest is the fact that the two longest Bi–Br bonds, to the two bridging bromines, are mutually *trans* which, as we shall see, is quite general and something to which we shall return later. Most simple bismuth bromide complexes contain octahedrally co-ordinated bismuth(III) with somewhat longer Bi–Br bonds, *e.g.* $[BiBr_6]^{3-}$ (2.822–2.865 Å),[7] $[\{(BiBr_5)^{2-}\}_n]$ (Bi–Br$_{terminal}$ 2.650–2.877, Bi–Br$_{bridging}$ 3.020–3.126 Å),[8] $[\{(BiBr_4)^{-}\}_n]$ (Bi–Br$_{terminal}$ 2.63–2.65, Bi–Br$_{bridging}$ 2.83–3.27 Å),[9] $[Bi_2Br_{11}]^{5-}$ (Bi–Br$_{terminal}$ 2.694–2.938, Bi–Br$_{bridging}$ 3.060–3.085 Å),[10] $[Bi_2Br_{10}]^{2-}$ (Bi–Br$_{terminal}$ 2.72–2.879, Bi–Br$_{bridging}$ 2.979–3.05 Å),[11] $[Bi_2Br_9]^{3-}$ (Bi–Br$_{terminal}$ 2.710–2.773, Bi–Br$_{bridging}$ 2.979–3.109 Å),[12] and $[Bi_4Br_{16}]^{4-}$ (Bi–Br$_{terminal}$ 2.663–2.694, Bi–Br$_{bridging}$ 2.914–3.156 Å).[13] Bismuth tribromide itself exists as two polymorphs: a molecular form with Bi–Br distances of 2.636–2.692 Å and longer bridging interactions at 3.246–3.397 Å, and a polymeric form containing octahedrally co-ordinated bismuth with Bi–Br distances in the range 2.79–2.84 Å.[14]

The iodide derivative, $[BiPhI_2(thf)]$ **2**, was prepared from $BiPh_3$ and two equivalents of I_2. The polymeric structure is similar to that of **1**, although the two compounds are not isomorphous. A view of the crystallographically independent unit (two monomers) is shown in Fig. 3 and a more extensive view of the polymeric solid-state structure is shown in Fig. 4. Selected bond lengths and angles are given in Table 3 and atomic positional parameters in Table 4. As with compound **1**, the co-ordination geometry around the bismuth centre is almost ideally square-based pyramidal with the phenyl group in the apical position and the bismuth essentially in the basal plane [Bi(1) 0.001(2) Å above, Bi(2) 0.006(2) Å below]. The shortest Bi–I bond lengths are to the terminal iodides [Bi(1)–I(1) 2.882(2), Bi(2)–I(2) 2.892(2) Å] with slightly longer distances to I(3) and I(4) which asymmetrically bridge between bismuth centres [Bi(1)–I(3) 3.056(2), Bi(2)–I(4) 3.079(2) Å]. The secondary Bi•••I interactions linking the monomer units into chains have the longest distances [Bi(1)–I(4a) 3.227(2), Bi(2)–I(3) 3.211(2) Å] and the co-ordination around each bismuth centre is completed by the oxygen atoms of thf molecules [Bi(1)–O(1) 2.808(17), Bi(2)–O(2) 2.813(18) Å]. For comparison, other bismuth iodide structures include $[BiI_6]^{3-}$ (Bi–I av. 3.075),[15] $[Bi_2I_9]^{3-}$ [Bi–I$_{terminal}$ 2.923(4), Bi–I$_{bridging}$ 3.249(5);[16] Bi–I$_{terminal}$ 2.920(2), Bi–I$_{bridging}$ 3.244(2) Å [17]], and $[Bi_3I_{12}]^{3-}$ (Bi–I$_{terminal}$ av. 2.910, Bi–I$_{bridging}$ av. 3.204 Å).[18] In all the above cases the bismuth atoms are octahedrally co-ordinated with Bi–I bond lengths on average slightly longer than those found in compound **2**. This co-ordination geometry is also found in bismuth triiodide itself for which the Bi–I distances are about 3.1 Å.[19]

An interesting comparison can be made between **1** and **2** with regard to the lengths of the intermolecular or secondary Bi–Br/I bonds. In **1** the relevant bond lengths in the Br–Bi••• Br unit

Table 4 Atomic coordinates (× 10^4) for compound **2**

Atom	*x*	*y*	*z*
Bi(1)	445(1)	8 041(1)	2 419(1)
Bi(2)	580(1)	12 992(1)	2 607(1)
I(1)	−1 109(3)	8 265(2)	1 025(1)
I(2)	2 269(3)	12 907(2)	3 967(1)
I(3)	−1 585(2)	10 385(2)	3 190(1)
I(4)	2 578(2)	15 378(1)	1 817(1)
O(1)	2 176(21)	7 959(22)	3 710(9)
C(1)	1 884(27)	8 718(31)	4 398(13)
C(2)	3 465(30)	8 768(31)	4 624(17)
C(3)	4 514(25)	7 788(27)	4 218(13)
C(4)	3 707(28)	7 219(33)	3 638(17)
O(2)	−1 321(23)	13 051(19)	1 372(9)
C(5)	−1 127(27)	14 160(23)	813(13)
C(6)	−2 829(28)	14 393(19)	600(15)
C(7)	−3 486(34)	12 963(24)	685(14)
C(8)	−2 816(28)	12 374(25)	1 395(14)
C(12)	−2 543(21)	5 964(17)	2 663(7)
C(13)	−3 477	4 924	3 046
C(14)	−3 170	4 452	3 780
C(15)	−1 931	5 020	4 132
C(16)	−997	6 061	3 749
C(11)	−1 304	6 533	3 014
C(22)	1 942(20)	11 188(18)	1 208(8)
C(23)	2 909	10 199	805
C(24)	4 179	9 518	1 142
C(25)	4 483	9 825	1 881
C(26)	3 515	10 813	2 284
C(21)	2 245	11 495	1 947

Table 5 Selected bond lengths (Å) and angles (°) for compound **3**

Bi(1)–I(1)	3.327(2)	Bi(1)–I(2)	3.285(2)
Bi(1)–I(3)	2.945(2)	Bi(1)–I(5)	2.948(2)
Bi(1)–C(11)	2.254(18)	Bi(2)–I(1)	3.288(2)
Bi(2)–I(2)	3.257(2)	Bi(2)–I(4)	2.972(2)
Bi(2)–I(6)	2.950(2)	Bi(2)–C(21)	2.266(18)
I(1)–Bi(1)–I(2)	80.4(1)	I(1)–Bi(1)–I(3)	170.9(1)
I(2)–Bi(1)–I(3)	91.8(1)	I(1)–Bi(1)–I(5)	96.1(1)
I(2)–Bi(1)–I(5)	172.3(1)	I(3)–Bi(1)–I(5)	91.1(1)
I(1)–Bi(1)–C(11)	90.6(5)	I(2)–Bi(1)–C(11)	92.4(4)
I(3)–Bi(1)–C(11)	94.3(5)	I(5)–Bi(1)–C(11)	94.5(4)
I(1)–Bi(2)–I(2)	81.3(1)	I(1)–Bi(2)–I(4)	92.8(1)
I(2)–Bi(2)–I(4)	173.4(1)	I(1)–Bi(2)–I(6)	171.8(1)
I(2)–Bi(2)–I(6)	91.4(1)	I(4)–Bi(2)–I(6)	94.3(1)
I(1)–Bi(2)–C(21)	92.3(5)	I(2)–Bi(2)–C(21)	91.5(4)
I(4)–Bi(2)–C(21)	91.8(4)	I(6)–Bi(2)–C(21)	91.7(4)
Bi(1)–I(1)–Bi(2)	77.3(1)	Bi(1)–I(2)–Bi(2)	78.3(1)

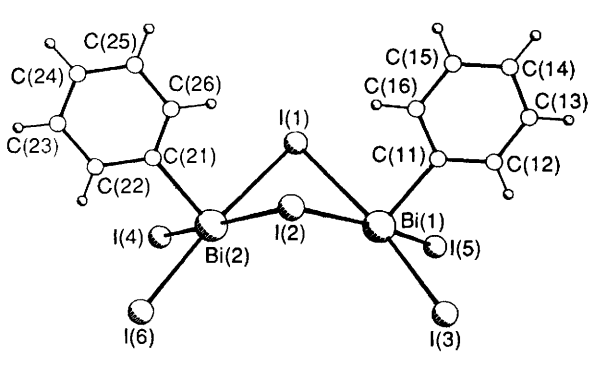

Fig. 5 A view of the structure of the dianion $[Bi_2Ph_2I_6]^{2-}$ in **3** showing the atom numbering scheme adopted

Table 6 Atomic coordinates (× 10^4) for compound **3**

Atom	*x*	*y*	*z*
Bi(1)	2552(1)	5497(1)	1752(1)
Bi(2)	2628(1)	2762(1)	2544(1)
I(1)	1416(1)	4355(1)	2319(1)
I(2)	3668(1)	4503(1)	3457(1)
I(3)	3713(1)	6264(1)	1379(1)
I(4)	1560(1)	1338(1)	1598(1)
I(5)	1498(1)	6133(1)	137(1)
I(6)	3848(1)	1559(1)	2747(1)
C(11)	2454(9)	6782(12)	2440(10)
C(12)	2332(10)	7672(13)	2034(12)
C(13)	2245(11)	8443(15)	2485(13)
C(14)	2243(11)	8359(16)	3248(13)
C(15)	2336(10)	7528(13)	3600(12)
C(16)	2415(10)	6719(13)	3171(11)
C(21)	2626(8)	2260(12)	3761(10)
C(22)	2701(9)	1309(12)	3953(10)
C(23)	2705(10)	1019(15)	4706(12)
C(24)	2637(10)	1644(14)	5242(12)
C(25)	2569(10)	2584(15)	5070(12)
C(26)	2568(9)	2878(13)	4312(10)
N(3)	179(8)	2057(11)	3481(9)
C(31)	483(14)	2996(19)	3823(17)
C(32)	−69(19)	3642(25)	3981(22)
C(33)	−446(13)	2084(19)	2682(14)
C(34)	−312(15)	2618(19)	2018(16)
C(35)	791(13)	1518(17)	3400(15)
C(36)	607(13)	553(17)	3089(14)
C(37)	−58(13)	1576(18)	4073(14)
C(38)	495(13)	1412(19)	4945(14)
N(4)	4849(8)	7771(11)	4129(10)
C(41)	4753(17)	6828(23)	3655(19)
C(42)	5443(13)	6221(18)	4032(15)
C(43)	5043(19)	7522(26)	5038(22)
C(44)	4442(16)	6872(22)	5141(19)
C(45)	4171(17)	8246(21)	3776(19)
C(46)	4171(15)	9220(18)	4230(16)
C(47)	5504(24)	8306(31)	4177(26)
C(48)	5324(17)	8677(22)	3256(17)
O(1)	2307(17)	9203(18)	403(17)
C(51)	1766(21)	9590(30)	−207(25)
C(52)	1138(21)	9134(30)	−275(26)
C(53)	2922(21)	9616(31)	577(25)
C(54)	3510(19)	9221(26)	1287(22)

are 2.825 and 3.038 Å the difference of which is 0.213 Å. In **2** the relevant average lengths for the I–Bi···I unit are 3.067 and 3.219 Å with a difference of 0.152 Å. Clearly in the iodide complex **2**, the primary and secondary Bi–I bonds are more nearly equal than the corresponding Bi–Br distances in **1**. This is consistent with a general observation first made by Alcock[2] that the primary and secondary bond lengths become closer as the electronegativity of the bridging atom decreases although the reason behind this observation is not entirely clear.

The bismuth–oxygen bond lengths in **1** and **2** are quite long indicating that the bismuth–thf interaction is fairly weak. For comparison, the average Bi–O distance in the three-co-ordinate monomeric alkoxide complex $[Bi(OC_6H_3Me_2\text{-}2,6)_3]$[20] is 2.091 Å. A more interesting comparison is the complex $[Bi(OSiPh_3)_3(thf)_3]$[21] for which the Bi–O(alkoxide) distance is 2.04(1) Å, even shorter than the previous example, whereas the Bi–O(thf) distance is almost 1 Å longer at 2.95(1) Å. This latter observation is quite general and has been discussed recently by Haaland.[22]

The reaction between **2** and $[NEt_4]I$ afforded, after work-up, a yellow crystalline material which was shown by X-ray crystallography to be $[NEt_4]_2[Bi_2Ph_2I_6]\cdot Et_2O$ **3**. A view of the phenyliodobismuthate dianion is shown in Fig. 5; selected bond lengths and angles are given in Table 5 and atomic positional parameters in Table 6. As is evident from Fig. 5, addition of iodide to **2** results in the dimeric, dianionic $[Bi_2Ph_2I_6]^{2-}$. Each bismuth atom has the same square-based pyramidal co-ordination geometry seen in **1** and **2** with apical phenyl groups and iodides in the basal plane; the bismuth atoms are 0.162(2) and 0.098(2) Å above their respective basal planes. The terminal

Table 7 Selected bond lengths (Å) and angles (°) for compound **5**

Bi–Br	2.741(1)	Bi–O	2.589(7)
Bi–C(11)	2.229(9)	Bi–C(21)	2.272(8)
Br–Bi–O	173.5(2)	Br–Bi–C(11)	93.2(2)
O–Bi–C(11)	80.8(3)	Br–Bi–C(21)	92.7(2)
O–Bi–C(21)	85.8(2)	C(11)–Bi–C(21)	98.2(3)

Table 9 Selected bond lengths (Å) and angles (°) for compound **6**

Bi–Br(1)	2.877(1)	Bi–Br(2)	2.863(1)
Bi–C(11)	2.276(3)	Bi–C(21)	2.260(3)
Br(1)–Bi–Br(2)	177.3(1)	Br(1)–Bi–C(11)	91.3(1)
Br(2)–Bi–C(11)	90.4(1)	Br(1)–Bi–C(21)	90.9(1)
Br(2)–Bi–C(21)	91.0(1)	C(11)–Bi–C(21)	95.9(1)

Table 8 Atomic coordinates (× 10^4) for compound **5**

Atom	*x*	*y*	*z*
Bi	1 171(1)	3 198(1)	7 077(1)
Br	3 117(1)	4 558(1)	7 805(1)
O	−768(6)	1 974(5)	6 584(5)
C(1)	−1 719(11)	1 697(13)	7 183(11)
C(2)	−2 210(24)	585(21)	6 799(18)
C(3)	−1 621(14)	235(10)	5 906(11)
C(4)	−834(9)	1 211(9)	5 688(8)
C(11)	637(8)	2 926(7)	8 689(6)
C(12)	−157(8)	3 652(8)	9 155(7)
C(13)	−565(9)	3 379(9)	10 086(7)
C(14)	−211(10)	2 333(9)	10 593(7)
C(15)	596(12)	1 610(9)	10 157(9)
C(16)	1 008(10)	1 917(8)	9 209(8)
C(21)	−16(7)	4 765(7)	6 608(5)
C(22)	350(9)	5 889(8)	6 908(7)
C(23)	−348(9)	6 829(8)	6 511(7)
C(24)	−1 389(8)	6 676(8)	5 833(7)
C(25)	−1 751(8)	5 569(8)	5 538(7)
C(26)	−1 064(8)	4 594(8)	5 917(6)

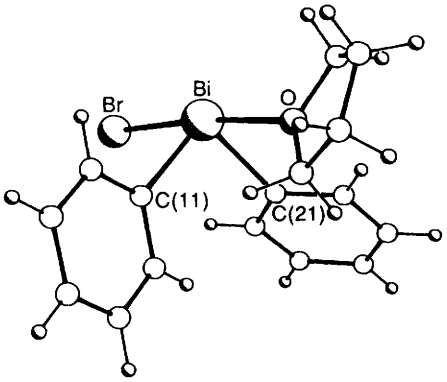

Fig. 6 A view of the structure of **5** showing the atom numbering scheme adopted

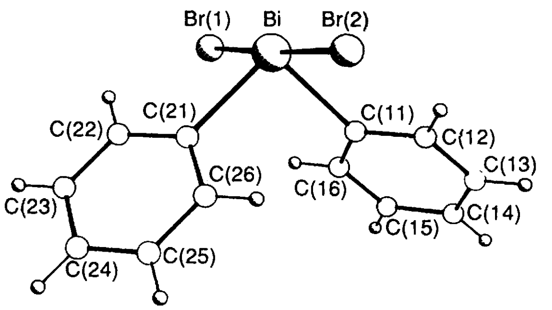

Fig. 7 A view of the structure of the anion $[BiPh_2Br_2]^-$ in **6** showing the atom numbering scheme adopted

Bi–I distances are the shortest (av. 2.954 Å) whilst the distances to the two symmetrically bridging iodides are longer (av. 3.289 Å), a feature in common with previously mentioned structures. The angles at the two bridging iodides are 77.3(1) and 78.3(1)° for I(1) and I(2) respectively. As is clear from Fig. 5, the Bi_2I_6 unit is not planar, the two square planes around each bismuth centre making an angle of 105.2° at the I(1)–I(2) vector. This is in contrast to the structures observed for the formally valence isoelectronic tellurium complex $[Te_2Ph_2I_6]$ (**4a**, **b**), described by Alcock and Harrison,[23] which exists as two polymorphs. The structures, shown diagrammatically below, can both be described as two edge-shared, square-based pyramids as is the case for **3** but in both the *cis* form (*cis* with respect to the phenyls), **4a**, and the *trans* form, **4b**, the Te_2I_6 unit is planar. The centrosymmetric *trans* structure is also found for the dianionic antimony complex $[Sb_2Ph_2Cl_6]^{2-}$ **4c** (pyridinium countercations) described recently by Hall and Sowerby.[24]

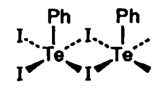

4a

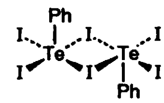

4b

Turning now to the diphenyl bismuth complexes, the structure of $[BiPh_2Br(thf)]$ **5**, obtained as yellow crystals from thf–hexane mixtures, is shown in Fig. 6. Selected bond lengths and angles are given in Table 7 and atomic positional parameters are presented in Table 8. The co-ordination geometry around the bismuth centre may be described as an equatorially vacant trigonal bipyramid (hereafter Ψtbp) with equatorial phenyl groups and the bromine and thf ligand in axial sites. The Bi–Br distance [2.741(1) Å] is longer than the terminal Bi–Br bond in **1** but shorter than the bridging Bi–Br bond in **1**. Also noteworthy is that the Bi–O(thf) bond length in **5** [2.589(7) Å] is shorter than the corresponding distance in **1** [Bi–O(thf) 2.671(8) Å]. As we shall discuss later, this structure is consistent with the argument that the acceptor orbital on the bismuth centre is the Bi–Br σ^* orbital. Thus shorter Bi–O donor bonds correlate with longer Bi–Br bonds due to greater population of this antibonding orbital. Also consistent with this bonding model is the observed *trans* disposition of the thf ligand to the Bi–Br bond, the relevant angle being O–Bi–Br 173.5(2)° (note that the deformation from 180° is towards rather than away from the phenyls) which suggests an alternative description of **5** as a trigonal pyramidal $BiPh_2Br$ molecule with a thf ligand bound *trans* to the bromine. The only other structure of a diarylbismuth halide of which we are aware was reported recently by Whitmire and Roesky and co-workers[25] namely $[Bi\{C_6H_2(CF_3)_3\text{-}2,4,6\}_2Cl]$ which is monomeric with no short intermolecular contacts.

Treatment of **5** with $[PPh_4]Br$ afforded, after work-up and crystallisation from CH_2Cl_2–hexane mixtures, crystals of the complex $[PPh_4][BiPh_2Br_2]$ **6**. A view of the structure of the $[BiPh_2Br_2]^-$ anion is shown in Fig. 7; selected bond lengths and angles are given in Table 9 and atomic positional parameters are presented in Table 10. The anion is monomeric and the geometry around the bismuth centre is Ψtbp with equatorial phenyls and axial bromides. The Bi–Br bond lengths are 2.877(1) and 2.863(1) Å, both similar to the distances found for the bridging bromides in **1**. The angles of most interest are those between the bromines [Br(1)–Bi–Br(2) 177.3(1)°] and between the phenyls [C(11)–Bi–C(21) 95.9(1)°] and we will comment on both in turn. The former angle is very close to the ideal value of 180°, as was also found for **5**, although in the case of **6** this bends away from the phenyls in contrast to the

Table 10 Atomic coordinates (× 10^4) for compound **6**

Atom	*x*	*y*	*z*
Bi	0	1096(1)	0
Br(1)	1742(1)	242(1)	−552(1)
Br(2)	1652(1)	2435(1)	596(1)
C(12)	−145(4)	2532(2)	−1064(2)
C(13)	−385	2905	−1687
C(14)	−739	2443	−2265
C(15)	−853	1608	−2220
C(16)	−613	1235	−1596
C(11)	−258	1697	−1018
C(22)	2009(3)	−427(2)	−24(2)
C(23)	3236	−866	−71
C(24)	4463	−468	−180
C(25)	4462	369	−242
C(26)	3235	808	−195
C(21)	2008	410	−86
P	3792(1)	−899(1)	2354(1)
C(32)	3210(3)	−2066(2)	3218(2)
C(33)	3544	−2612	3744
C(34)	4930	2646	4111
C(35)	5981	−2133	3953
C(36)	5646	−1587	3428
C(31)	4261	1553	3061
C(42)	2455(4)	546(2)	2037(1)
C(43)	1591	1198	2134
C(44)	1012	1248	2714
C(45)	1297	645	3197
C(46)	2161	−6	3100
C(41)	2740	−56	2520
C(52)	5781(4)	−710(2)	1513(2)
C(53)	6995	−365	1335
C(54)	7793	198	1754
C(55)	7377	416	2352
C(56)	6164	71	2530
C(51)	5366	492	2110
C(62)	1299(4)	−1319(2)	1494(2)
C(63)	431	−1852	1073
C(64)	1001	−2567	874
C(65)	2439	2748	1096
C(66)	3308	2215	1517
C(61)	2738	−1500	1716

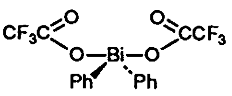

7

situation observed for **5**. While it is unlikely that this small distortion has much significance, the near linearity certainly does. There are, in fact, very few reported structures of anionic, ten-electron, four-co-ordinate bismuth compounds. Of particular relevance is a compound reported by Barton *et al.*[26] namely $[BiPh_2(O_2CCF_3)_2]^-$ **7** the structure of which is shown above. This is similar in most respects to **6**; the angle between the axial oxygens is 171.8° and that between the phenyl *ipso* carbons is 94.8°. This is the expected structure for such compounds based on valence-shell electron-pair repulsion (VSEPR) arguments but we have also characterised the complexes $[BiCl_2(ML_n)_2]^-$ [ML_n = $Fe(CO)_2(\eta-C_5H_5)$ or $Mo(CO)_3(\eta-C_5H_5)$][27] for which a distortion towards tetrahedral geometry is seen. This may result from π-donation to the bismuth centre from the metal fragments as we shall discuss later.

The angles between the *ipso* carbons in **5**–**7** range from about 94 to 98°, significantly less than the ideal value of 120°. Attention has been drawn to this fact in a recent article by Calderazzo *et al.*[28] in which the structure of the related anionic antimony complex $[SbPh_2Cl_2]^-$ **8** is described. These authors report the structure of $[Co(\eta-C_5H_5)_2][SbPh_2Cl_2]$ **8a**, the antimonate anion of which is very similar to the bismuth analogue in **6** and for which the angle between the two *ipso* carbons is 97.3(7)°. An essentially identical angle has been found in the $[NMe_4]$ derivative **8b** by Hall and Sowerby[24] [97.5(3)°] both of which are a little over 1° greater than the angle in **6**. Also of interest are a number of neutral tellurium(IV) compounds, namely $[TePh_2X_2]$ (X = F, Cl, Br or I). All have structures similar to **6** and **8** with equatorial phenyls and axial halides and the following bond angles (X–Te–X, C–Te–C): X = F,[29] 173.1(1), 96.9(1); X = Cl,[30] 175.5(1), 99.0(3); X = Br,[31] 177.9(2), 94.4(12); X = I,[23] 174.7 (av.), 95.4 (av.)°. Acute interbond angles are common in the structural chemistry of the heavier main-group elements and a trend is often observed wherein the bond angles decrease as the group is descended. The case in question here, ten-electron AB_4 (where A is the central atom Bi, Sb or Te in the examples quoted above), is dealt with explicitly by Gimarc and Khan.[32] They show that the deviation from tetrahedral geometry is driven by stabilisation and hybridisation of the lone pair (to which the central atom contribution is a pure s orbital) by mixing with the pseudo-equatorial A–B σ and σ* orbitals which introduce p character from A into the highest-occupied molecular orbital (HOMO) (see Scheme 1). This stabilisation is enhanced when the central A atom is less electronegative. Therefore on descending a group (*e.g.* N, P, As, Sb, Bi), the fall in electronegativity would be expected to result in decreasing B–A–B angles both in trigonal-pyramidal AB_3 species[33] and in the equatorial sites of ten-electron AB_4 species.

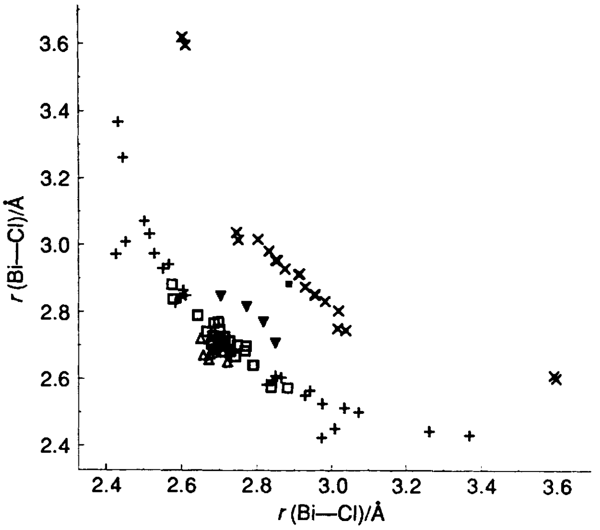

Fig. 8 Cl ··· Bi and Bi–Cl distances (Å) for *trans*-Cl ··· Bi–Cl bonds in bismuth(III) complexes determined by crystallography. Symbols are used to indicate: (*i*) the presence of one or more other chlorine ligands *cis* to the two *trans* chlorines (■, □, +); (*ii*) that neither of the two *trans* chlorines is bridging to a second metal (▼, □, △); (*iii*) that exactly one of the two *trans* chlorines is bridging to a second metal (+); (*iv*) that both of the two *trans* chlorines are bridging to other metals (■, ×); (*v*) the presence of one or more transition-metal fragment ligands *cis* to the two *trans* chlorines (▼, ×)

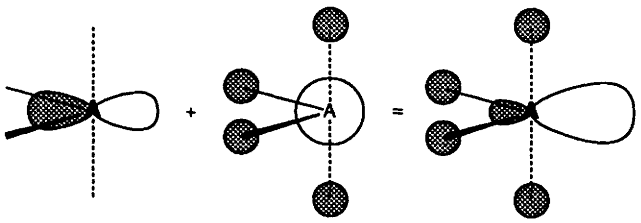

Scheme 1

We now turn to a more general discussion of the factors affecting primary *vs.* secondary bond distances in these and related compounds. Figs. 8, 9 and 10 show plots of Bi–X distances in species containing *trans* X–Bi ··· X systems (where X = Cl, Br or I, and which have X–Bi ··· X angle > 140°) taken

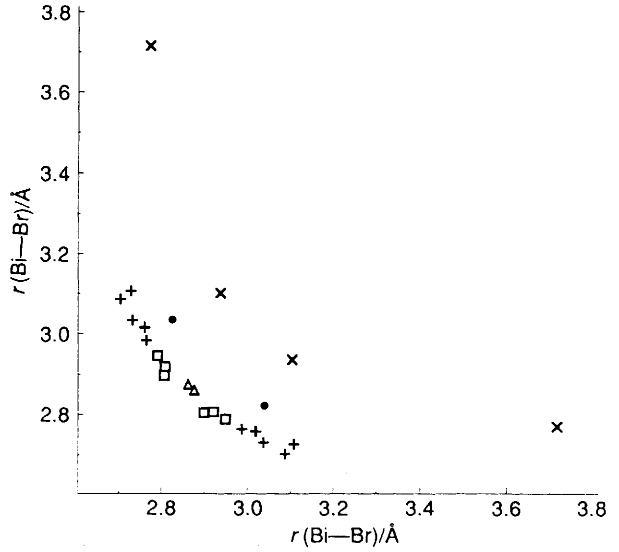

Fig. 9 Br ··· Bi and Bi–Br distances (Å) for *trans*-Br ··· Bi–Br bonds in bismuth(III) complexes determined by crystallography. Symbols are used to indicate: (*i*) the presence of one or more other bromine ligands *cis* to the two *trans* bromines (□, +); (*ii*) that neither of the two *trans* bromines is bridging to a second metal (□, △); (*iii*) that exactly one of the two *trans* bromines is bridging to a second metal (+); (*iv*) that both of the two *trans* bromines are bridging to other metals (●, ×); (*v*) the presence of one or more transition-metal fragment ligands *cis* to the two *trans* bromines (×); (*vi*) the presence of no bromine or transition-metal fragment ligands *cis* to the two *trans* bromines (×)

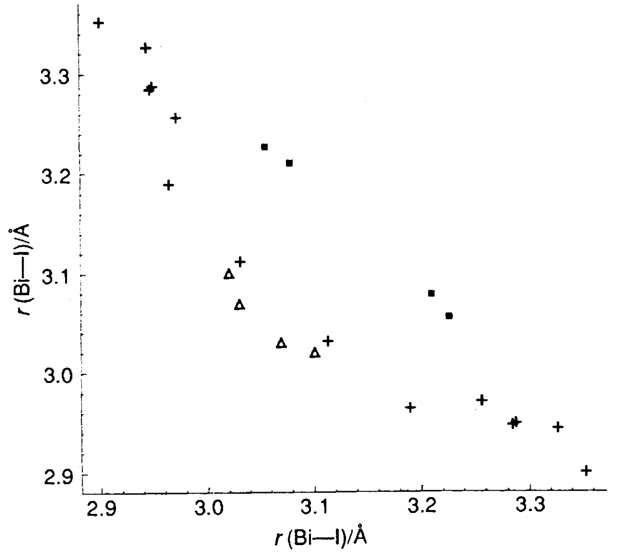

Fig. 10 I ··· Bi and Bi–I distances (Å) for *trans*-I ··· Bi–I bonds in bismuth(III) complexes determined by crystallography. Symbols are used to indicate: (*i*) the presence of one or more other iodine ligands *cis* to the two *trans* iodines (+); (*ii*) that neither of the two *trans* iodines is bridging to a second metal (△); (*iii*) that exactly one of the two *trans* iodines is bridging to a second metal (+); (*iv*) that both of the two *trans* iodines are bridging to other metals (■)

from the Cambridge Structural Database[34] of July 1991 with the restriction that the crystallographic *R* factor be less than 0.07 (and from our own work,[35] and ref. 36). As we noted previously in the case of X = Cl,[35] each of the plots show an overall curvature and may be taken to illustrate the effect of primary and secondary interactions on one another. Taking the Bürgi–Dunitz[37] view of such plots, the distribution of points maps the S_N2 displacement of one halide atom by another in these bismuth(III) species, as illustrated in Scheme 2. The form of this plot is broadly similar to those obtained for other associative nucleophilic substitution models studied in this way showing concave curvature with the sums of interatomic distances at the mid-point of the symmetrical curves lower than at the extremities.[38] However the behaviour in these plots is clearly complex, and most strikingly so for the case X = Cl for which the data are most extensive. There appear to be two distinct, near parallel curves of points, one which passes through a central point where both Bi ··· Cl distances are *ca.* 2.9 Å and the other (more populated) passing through a central point where both Bi ··· Cl distances are *ca.* 2.7 Å. The extremes of these curves are also apparently different, for the outer curve the short Bi ··· Cl distance apparently asymptotically approaches *ca.* 2.6 Å as the longer distance tends to non-interacting values (>3.6 Å), for the inner curve the short Bi–Cl distance apparently asymptotically approaches *ca.* 2.4 Å. Similar behaviour, albeit much less clearly defined, is apparent for the more sparse plots for the *trans*-Br–Bi ··· Br and *trans*-I–Bi ··· I systems (see Figs. 9 and 10). In the case of X = Br the inner curve is centred at Bi ··· Br *ca.* 2.85 Å and asymptotically approaches *ca.* 2.6 Å, while the putative outer curve is apparently centred on *ca.* 3.05 Å and approaches 2.75 Å in the asymmetric limit. For Bi–I distances, although the two curves are still less well defined, one might suggest that the inner curve is centred on *ca.* 3.05 Å, while the outer is barely discernible but may be centred at 3.15 Å.

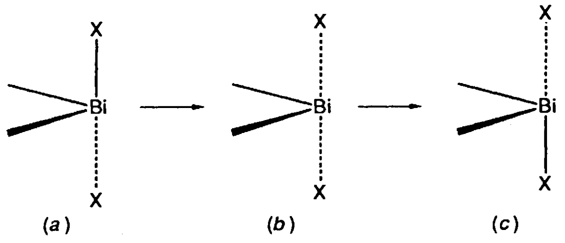

Scheme 2

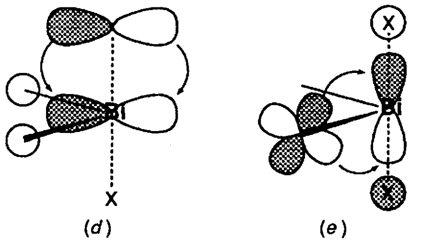

Scheme 3

We have considered a variety of causes for the apparently dichotomous behaviour of the *trans*-X–Bi ··· X distances. Among the possibilities are the *cis* influences of the other (non-X) substituents at the bismuth and the variation in the *trans* influence of the X atoms caused by their being either bridging (*e.g.* to other bismuth atoms) or terminal. Two types of possible *cis* influences might be envisaged: (1) the capacity of electronegative substituents (*e.g.* X, OR) to cause shortening of Bi–X bonds *cis* to themselves through negative hyperconjugation [see Scheme 3 interaction (*d*)]; (2) the effect of π-donating (notably transition-metal) substituents to induce Bi–X bond lengthening *cis* to themselves [see Scheme 3 interaction (*e*)]. The first of these interactions would be the result of improved Bi–X π bonding resulting from overlap of lone pairs on the X atoms with the Bi–Z σ^* orbital(s) (Z = electronegative substituent). The second possible interaction involves *cis* π-donor ligands [*e.g.* transition-metal-ligand fragments such as $Fe(CO)_2(\eta\text{-}C_5H_5)$] which push electron density into the Bi–X σ^* orbital thereby weakening and lengthening the Bi–X distance. The effect of additional bonds at the X ligands, as when the halide atoms bridge between two (or more) bismuth atoms was also considered. Clearly highly asymmetric X–Bi ··· X systems are to be expected when one X is terminal and the other bridging, in contrast, in structures where both X atoms are terminal the X–Bi–X system would be expected to be more

Table 11 Crystallographic data[a]

	1	**2**	**3**	**5**	**6**
Formula	$C_{10}H_{13}BiBr_2O$	$C_{10}H_{13}BiI_2O$	$C_{32}H_{60}Bi_2I_6N_2O$	$C_{16}H_{18}BiBrO$	$C_{36}H_{30}BiBr_2P$
M	518.0	612.0	1668.2	515.2	862.4
Crystal system	Monoclinic	Triclinic	Monoclinic	Monoclinic	Monoclinic
Space group	$P2_1/c$	$P\bar{1}$	$P2_1/c$	$P2_1/n$	Cc
a/Å	8.185(3)	8.308(4)	20.670(4)	11.128(2)	9.523(1)
b/Å	9.282(5)	9.657(5)	14.287(3)	11.503(2)	16.599(2)
c/Å	17.146(6)	17.567(8)	17.654(4)	12.747(2)	20.391(3)
α/°		87.44(4)			
β/°	94.59(4)	83.95(4)	113.80(1)	96.92(2)	100.46(1)
γ/°		88.05(3)			
U/Å^3	1298.5	1399.4	4770.0	1619.8	3169.7
D_c/g cm^{-3}	2.649	2.904	2.323	2.112	1.807
μ/mm^{-1}	19.6	16.9	11.2	13.3	8.1
F(000)	936	1080	3032	960	1656
Crystal size (mm)	0.27 × 0.27 × 0.42	0.13 × 0.27 × 0.37	0.17 × 0.21 × 0.42	0.31 × 0.42 × 0.73	0.27 × 0.35 × 0.42
Transmission	0.003–0.015	0.007–0.027	0.065–0.101	0.004–0.017	0.028–0.058
Reflections measured	6210	7725	10 283	4160	5575
Unique reflections	2282	4884	8395	2858	5575
Observed reflections	2004	3759	5057	2415	5275
R_{int}	0.032	0.056	0.054	0.024	—
Method of solution	Patterson	Direct methods	Direct methods	Direct methods	Patterson
Extinct. parameter, x	0	0	0	0	1.4(4) × 10^{-7}
Weighting scheme:					
A_1	+44	+394	+98	−108	−53
A_2	+1362	−755	−651	+1309	+453
A_3	−696	+8488	+903	−1222	−9
A_4	−344	−1260	−60	+157	+67
A_5	+336	+933	−44	−35	+5
A_6	−1437	+483	+438	−1493	−584
No. of parameters	127	129	228	172	288
R	0.050	0.106	0.065	0.043	0.031
$R' = (\Sigma w\Delta^2/\Sigma wF_o^2)^{\frac{1}{2}}$ [b]	0.038	0.137	0.050	0.046	0.035
Slope of normal probability plot	0.97	0.99	0.92	0.76	1.06
Maximum, mean Δ/σ	0.005, 0.001	0.008, 0.001	0.040, 0.011	0.006, 0.001	0.017, 0.003
Max., min. $\Delta\rho$/e Å^{-3}	4.12, −1.34	7.60, −4.20	1.83, −1.13	2.25, −1.00	2.40, −3.04

[a] Details in common: $Z = 4$, $2\theta_{max} = 50°$. [b] $\Delta = ||F_c| - |F_o||$.

nearly symmetric. Inspection of Fig. 8 shows strong evidence that these latter expectations are indeed fulfilled with complexes having two terminal *trans* chlorines (points with symbols □, △) clustered near to the centre of the curve, where the two Bi–Cl distances are equal. The common feature of all the points lying on the outer curve is that they contain π-donor groups *cis* to the pair of Bi–Cl vectors *and* that both chlorines are in bridging sites. The π-donor groups are either transition-metal fragments (symbol ×) or a π-bound arene (■). The small group of points (▼) which have both chlorines terminal and two *cis* metal ligands lie between the two major curves. Similar comments apply to the Br–Bi–Br plot with the inner curve being composed of structures with one or no bridging bromine atoms, and the other points deviating from the curve (due to complex **1**, points ●, and the complex $[BiBr\{Mo(CO)_3(\eta\text{-}C_5H_5)\}_2]$,[35] points ×) having both bromines bridging, and having σ-aryl and metal fragments *cis* to the Br–Bi–Br unit (both of which are potential π donors, albeit rather weak in the case of the σ aryl). In both Figs. 8 and 9 the number of halides *cis* to the X–Bi–X unit appears to have no substantial influence on the Bi–X distances.

The conclusion to be tentatively drawn from these observations is that the effect of both chlorines being in bridging sites and the π-donor ability, and especially that of the transition-metal fragments, are the key factors in determining the position of points relative to the two main curves in these plots. In practice it seems likely that there exist a continuum of parallel curves between (and perhaps beyond) the extremes most clearly exemplified in the Cl–Bi–Cl plot. Using molecular-orbital methods, we will explore this suggestion, the relationship of these geometric deformations to others (*e.g.* variations in the X–Bi···X bond angle), and the differences between the behaviour of these systems and those with similar stoichiometry but differing electron count in a future paper.

Experimental

General Procedures.—All reactions were performed using standard Schlenk techniques under an atmosphere of dry, oxygen-free dinitrogen. All solvents were distilled from appropriate drying agents immediately prior to use (sodium–benzophenone for thf, Et_2O and hexanes; CaH_2 for MeCN and CH_2Cl_2). $BiBr_3$, BiI_3 and $BiPh_3$ (all 99%+) were procured commercially and used without further purification.

Preparations.—The preparations described below are all based on literature methods which are listed and referenced in ref. 1.

$[BiPhBr_2(thf)]$ **1**. A sample of $BiPh_3$ (1.072 g, 2.437 mmol) was added to a stirred, yellow solution of $BiBr_3$ (2.187 g, 4.875 mmol) in Et_2O (20 cm^3) at room temperature resulting in the immediate formation of a yellow precipitate. After 30 min, the solvent was removed by vacuum yielding **1** as a yellow powder (2.913 g, 89%). Pale yellow X-ray quality crystals of **1** were obtained by solvent diffusion from thf (5 cm^3)–hexanes (30 cm^3) mixtures at −25 °C over a period of days. At room temperature, these crystals readily lost solvent but were stable for much longer periods at −40 °C.

$[BiPhI_2(thf)]$ **2**. A solution of I_2 (0.306 g, 1.204 mmol) in Et_2O (10 cm^3) was added to a stirred solution of $BiPh_3$ (0.265 g, 0.602 mmol) in Et_2O (10 cm^3) at room temperature which resulted in the immediate formation of an orange precipitate. After 15 min all volatiles were removed by vacuum resulting in a red-orange powder (0.295 g, 91%). Bright orange X-ray quality crystals of **2** were obtained by solvent diffusion from thf (5 cm^3)–hexane (30 cm^3) mixtures at −25 °C over a period of days. At room temperature, these crystals readily lost solvent but were stable for much longer periods at −40 °C.

$[NEt_4]_2[Bi_2Ph_2I_6]$ **3**. A sample of $BiPhI_2$ (0.295 g, 0.546 mmol) and $[NEt_4]I$ (0.140 g, 0.546 mmol) were dissolved in thf (10 cm^3) and the resulting orange solution stirred for 24 h. After this time all volatiles were removed by vacuum resulting in an orange powder which was redissolved in MeCN (5 cm^3) and crystallised by solvent diffusion using an overlayer of Et_2O (20 cm^3) at −25 °C over a period of days. This procedure afforded orange X-ray quality crystals of **3**.

$[BiPh_2Br(thf)]$ **5**. A solution of $BiBr_3$ (0.262 g, 0.584 mmol) in Et_2O (10 cm^3) was added to a stirred solution of $BiPh_3$ (0.514 g, 1.168 mmol) in Et_2O (20 cm^3) at room temperature resulting in the formation of a yellow precipitate. After 15 min the solvent was removed by vacuum resulting in a pale yellow powder. Pale yellow X-ray quality crystals of **5** were obtained by solvent diffusion from thf (5 cm^3)–hexane (30 cm^3) mixtures at −25 °C over a period of days. At room temperature, these crystals readily lost solvent but were stable for much longer periods at −40 °C.

$[PPh_4][BiPh_2Br_2]$ **6**. A sample of $BiPh_2Br$ (0.238 g, 0.537 mmol) and $[PPh_4]Br$ (0.225 g, 0.537 mmol) were dissolved in CH_2Cl_2 (10 cm^3) and the resulting mixture stirred for 24 h after which time the reaction flask contained a pale yellow solution and a white precipitate. After allowing the solid to settle, the solution was transferred to another flask and hexane (30 cm^3) added as an overlayer. X-Ray quality crystals were obtained by solvent diffusion at −25 °C over a period of days.

X-Ray Crystallography.—Crystal data are given in Table 11, with other pertinent information concerning data collection and structure determination. Measurements for compounds **1**, **2**, **5** and **6** were made at 240 K, and for **3** at 295 K on a Stoe-Siemens diffractometer, with graphite-monochromated Mo-Kα radiation (λ = 0.710 73 Å). Unit-cell parameters were refined from 2θ values (20–25°) of 32 reflections measured at ±ω in each case. Data were collected in a ω–θ scan mode with variable scan width and time and with on-line profile fitting.[39] No significant variation in intensity was observed for three periodically-measured standard reflections in each case. Data were corrected for Lorentz/polarisation effects and absorption (semi-empirically).

The structures were solved[40] and refined by blocked-cascade least squares on *F*, with weighting[41] [$w^{-1} = \sigma^2(F) = \sigma_c^2(F) + A_1 + A_2G + A_3G^2 + A_4S + A_5S^2 + A_6GS$, where $G = F_o/F_{max}$, $S = \sin\theta/\sin\theta_{max}$]. Atomic scattering factors were taken from ref. 42. Refinement included an isotropic extinction parameter x [$F_c' = F_c/(1 + xF_c^2/\sin 2\theta)^{\frac{1}{4}}$], and anisotropic thermal motion parameters for all atoms except C and H in **2** and **3**, and all non-hydrogen atoms in **1**, **5** and **6**. Hydrogen atoms were constrained on idealised positions [C–H 0.96 Å, H–C–H 109.5°, aromatic H on ring-angle external bisectors, $U(H) = 1.2U_{eq}(C)$]. In each case, the largest residual-difference electron-density peaks were located near the Bi atoms.

Additional material available from the Cambridge Crystallographic Data Centre comprises H-atom coordinates, thermal parameters and remaining bond lengths and angles.

Acknowledgements

We thank the SERC for financial support and BP Research (Sunbury) for a CASE award (to G. A. F.). N. C. N. thanks the Royal Society for additional supporting funds.

References

1 L. D. Freedman and G. O. Doak, *Chem. Rev.*, 1982, **82**, 15, and refs. therein.

2 N. W. Alcock, *Adv. Inorg. Chem. Radiochem.*, 1972, **15**, 1.

3 H. Gilman and H. L. Yablunky, *J. Am. Chem. Soc.*, 1941, **63**, 207; H. Gilman and H. L. Yale, *Chem. Rev.*, 1942, **30**, 281.

4 D. M. Hawley and G. Ferguson, *J. Chem. Soc. A*, 1968, 2059.

5 F. Calderazzo, A. Morvillo, G. Pelizzi and R. Poli, *J. Chem. Soc., Chem. Commun.*, 1983, 507.

6 J. M. Cassidy and K. H. Whitmire, *Inorg. Chem.*, 1991, **30**, 2788.

7 W. G. McPherson and E. A. Meyers, *J. Phys. Chem.*, 1968, **72**, 3117; F. Lazarini, *Acta Crystallogr., Sect. B*, 1978, **34**, 2288.

8 W. G. McPherson and E. A. Meyers, *J. Phys. Chem.*, 1968, **72**, 532.

9 B. K. Robertson, W. G. McPherson and E. A. Meyers, *J. Phys. Chem.*, 1967, **71**, 3531.

10 J. Matuszewski, R. Jakubas, L. Sobczyk and T. Glowiak, *Acta Crystallogr., Sect. C*, 1990, **46**, 1385.

11 F. Lazarini and I. Leban, *Acta Crystallogr., Sect. B*, 1980, **36**, 2745; F. Lazarini, *Acta Crystallogr., Sect. B*, 1977, **33**, 1954.

12 F. Lazarini, *Acta Crystallogr., Sect. B*, 1977, **33**, 2686, 2961.

13 A. L. Rheingold, A. D. Uhler and A. G. Landers, *Inorg. Chem.*, 1983, **22**, 3255.

14 H. von Benda, *Z. Krystallogr.*, 1980, **151**, 271.

15 F. Lazarini, *Acta Crystallogr., Sect. B*, 1977, **33**, 1957.

16 O. Lindqvist, *Acta Chem. Scand.*, 1968, **22**, 2943.

17 B. Chabot and E. Parthe, *Acta Crystallogr., Sect. B*, 1978, **34**, 645.

18 U. Geiser, E. Wade, H. H. Wang and J. M. Williams, *Acta Crystallogr., Sect. C*, 1990, **46**, 1547.

19 J. Trotter and T. Zobel, *Z. Kristallogr.*, 1966, **123**, 67.

20 W. J. Evans, J. H. Hain and J. W. Ziller, *J. Chem. Soc., Chem. Commun.*, 1989, 1628.

21 M.-C. Massiani, R. Papiernik, L. G. Hubert-Pfalzgraf and J.-C. Daran, *Polyhedron*, 1991, **10**, 437.

22 A. Haaland, *Angew. Chem., Int. Ed. Engl.*, 1989, **28**, 992.

23 N. W. Alcock and W. D. Harrison, *J. Chem. Soc., Dalton Trans.*, 1984, 869.

24 M. Hall and D. B. Sowerby, *J. Organomet. Chem.*, 1988, **347**, 59.

25 K. H. Whitmire, D. Labahn, H. W. Roesky, M. Noltemeyer and G. M. Sheldrick, *J. Organomet. Chem.*, 1991, **402**, 55.

26 D. H. R. Barton, B. Charpiot, E. T. H. Dau, W. B. Motherwell, C. Pascard and C. Pichon, *Helv. Chim. Acta*, 1984, **67**, 586.

27 W. Clegg, N. A. Compton, R. J. Errington, G. A. Fisher, D. C. R. Hockless, N. C. Norman and A. G. Orpen, *Polyhedron*, 1991, **10**, 123.

28 F. Calderazzo, F. Marchetti, F. Ungari and M. Wieber, *Gazz. Chim. Ital.*, 1991, **121**, 93.

29 F. J. Berry and A. J. Edwards, *J. Chem. Soc., Dalton Trans.*, 1980, 2306.

30 N. W. Alcock and W. D. Harrison, *J. Chem. Soc., Dalton Trans.*, 1982, 251.

31 G. D. Christofferson and J. D. McCullough, *Acta Crystallogr.*, 1958, **11**, 249.

32 B. M. Gimarc and S. A. Khan, *J. Am. Chem. Soc.*, 1978, **100**, 2340.

33 T. A. Albright, J. K. Burdett and M. H. Whangbo, *Orbital Interactions in Chemistry*, Wiley-Interscience, New York, 1985; B. M. Gimarc, *Molecular Structure and Bonding*, Academic Press, New York, 1979.

34 F. H. Allen, O. Kennard and R. Taylor, *Acc. Chem. Res.*, 1983, **16**, 146.

35 W. Clegg, N. A. Compton, R. J. Errington, G. A. Fisher, D. C. R. Hockless, N. C. Norman, N. A. L. Williams, S. E. Stratford, S. J. Nichols, P. S. Jarrett and A. G. Orpen, *J. Chem. Soc., Dalton Trans.*, 1992, 193 and refs. therein.

36 G. R. Willey, H. Collins and M. G. B. Drew, *J. Chem. Soc., Dalton Trans.*, 1991, 961.

37 H. B. Bürgi and J. D. Dunitz, *Acc. Chem. Res.*, 1983, **16**, 153.

38 See, for example, K. B. Dillon, A. W. G. Platt, A. Schmidpeter, F. Zwaschka and W. S. Sheldrick, *Z. Anorg. Allg. Chem.*, 1982, **488**, 7.

39 W. Clegg, *Acta Crystallogr., Sect. A*, 1981, **37**, 22.

40 G. M. Sheldrick, SHELXTL: an integrated system for solving, refining, and displaying crystal structures from diffraction data, University of Göttingen, 1985, revision 5.

41 Wang Hong and B. E. Robertson, *Structure and Statistics in Crystallography*, ed. A. J. C. Wilson, Adenine Press, New York, 1985, pp. 125–136.

42 *International Tables for X-Ray Crystallography*, Kynoch Press, Birmingham, 1974, vol. 4, pp. 99, 149.

Received 13*th February* 1992; *Paper* 2/00783E